

Determining the Stability and Control Characteristics of High-Performance Maneuvering Aircraft Using High-Resolution CFD Simulation with and without Moving Control Surfaces

James D. Clifton^{*}, C. Justin Ratcliff[†], David J. Bodkin[‡], John P. Dean[§]
United States Air Force SEEK EAGLE Office, Eglin AFB, FL 32542

This paper discusses the development of a computational approach for accurately determining static and dynamic stability and control characteristics of USAF high-performance fighter aircraft. A graduated approach is used to incrementally add Computational Fluid Dynamics (CFD) simulation capability using DoD HPC resources. Static simulations, prescribed motion flight test maneuvers, and System Identification (SID) of CFD have been accomplished and show good predictive capabilities when tested against wind tunnel data and Lockheed Martin's performance data. The focus of this paper is the modeling and simulation of moving control surfaces in CFD and calculating aircraft/store increment data for use in flight test preparation and analysis. Flight test maneuvers were performed in CFD using both flight test data and maneuver response data from Lockheed Martin's 6-DOF and flying qualities simulation, ATLAS. Non-flyable, computational training maneuvers designed to capture both static and dynamic aerodynamics as well as aiding discovery of envelope-limiting, nonlinear aerodynamic phenomena are simulated as forced rotational and/or translational oscillations about one or more axes. Nonlinear, reduced-order aerodynamic models of USAF fighter aircraft with and without stores have been generated through SID of the aforementioned computational training maneuvers. A full-scale F-16C aircraft with movable control surfaces is modeled using unstructured viscous over-set grids and the *Cobalt* solver. Current work to employ external feedback control to manipulate movable control surfaces and boundary conditions in CFD is discussed. The necessity of DoD HPC resources to support the USAF T&E community in gathering critical data in a timely manner to rapidly deliver capability to the warfighter is reaffirmed.

1. Introduction

PRACTICALLY every fighter program since 1960 has had costly nonlinear aerodynamic or fluid-structure interaction issues discovered in flight test (FT). The main reason for these “failures” is that the predictive methods used were not able to reveal the onset and nature of the problems early in the design phase. To keep the budget overshoot under control, fixes tend to be *ad hoc* and are applied without a sound basis of fundamental understanding of the physics concerned. Unfortunately, in future aircraft designs, the problems will only become more complex as thrust vectoring, active aeroelastic structures, and other related technologies are implemented for stability and control (S&C) augmentation. Unmanned combat vehicles will operate in flight regimes where highly unsteady, nonlinear, and separated flow characteristics dominate since there are no man-rating requirements [1]. Similar problems persist throughout the life-cycle of an aircraft as user requirements expand beyond Initial Operational Capability (IOC). Integration of new stores (e.g. weapons, pods, suspension equipment, countermeasures) on existing platforms poses unique aircraft-store compatibility challenges for a wide range of engineering disciplines, including stability and control. In order to reduce the risk to aircrews during testing and the costs incurred by extensive wind tunnel and flight tests, it would be helpful to have a tool which enabled engineers and designers to analyze and evaluate the non-linear, flight-dynamic behavior of the aircraft and/or associated armament both early in the design phase and throughout sustainment.

^{*} Team Lead, Stability and Control/Handling Qualities, USAF SEEK EAGLE Office, Eglin AFB, FL

[†] Engineer, Stability and Control/Handling Qualities, USAF SEEK EAGLE Office, Eglin AFB, FL

[‡] Engineer, Stability and Control/Handling Qualities, USAF SEEK EAGLE Office, Eglin AFB, FL

[§] Chief, Interference Mechanics Division, USAF SEEK EAGLE Office, Eglin AFB, FL

The present paper discusses static, time-accurate and rigid body, prescribed motion maneuvers using CFD both with and without moving control surfaces on the A-10C Thunderbolt II, F-16C Falcon, and F-22 Raptor from an S&C perspective. All runs were conducted on DoD High Performance Computing (HPC) resources. Static, time-accurate CFD simulations of an A-10C in both the clean aircraft configuration (no external stores) as well as configurations with an external fuel tank were performed. Static, time-accurate CFD simulations of an F-16C in an Air-to-Ground configuration with AGM-154 JSOWs are compared to GBU-39 SDB wind tunnel data. Static, time-accurate CFD simulations of an F-22 in both the clean aircraft configuration as well as configurations with external fuel tanks were performed. Longitudinal and lateral-directional static stability were investigated at select Mach and altitude conditions. Results from prior wind tunnel (WT) tests and Lockheed Martin (LM) performance data served as validation data. Nonlinear, reduced-order, aerodynamic models of the A-10C, F-16C, and F-22 have been generated through system identification (SID) of rigid body, prescribed motion computational training maneuvers using methods previously documented [2] and new methods described below. The resulting SID models were tested against wind tunnel data; Lockheed Martin performance data; static, time-accurate CFD simulations; and CFD simulations of prescribed motion flight-test maneuvers. Rigid body, prescribed motion flight test maneuvers with moving control surfaces performed in CFD with an F-16C in the clean configuration were compared to the corresponding F-16 ATLAS simulation. The CFD simulations performed investigated longitudinal and lateral-directional static stability. Aircraft flight control laws and 6-DoF capability are being developed in parallel to be utilized with CFD on HPC machines. CFD simulations serving as a test for integrating these capabilities are discussed.

Though the production-level application of CFD to S&C is still in its early stages, CFD has been shown in previous papers to be a realistic modeling and simulation method capable of providing accurate S&C data for aircraft-store certification activities. Certification activities are typically accomplished by analogy, with flight testing and wind tunnel testing performed when stores are sufficiently different from previously cleared stores. This approach works with current legacy aircraft. However, 5th generation aircraft, such as the F-22 and the F-35, will require much more flight testing and wind tunnel testing. Current Modeling and Simulation (M&S) tools are inadequate to predict S&C-related aerodynamic instabilities resulting in increased risk and cost to FT and WT test activities as well as reduced capability to the warfighter. Rapid generation of aerodynamic databases of new aircraft-store configurations for maneuver response simulations and analysis, including envelope expansion and elimination of unnecessary restrictions due to insufficient funds and understanding of S&C related aerodynamic phenomena, is essential. In order to rapidly deliver greater combat capability to the warfighter at reduced risk and cost, integration of advanced CFD methods run on DoD HPC resources will be necessary to optimize available resources for flight test and wind tunnel test of new aircraft and weapons systems.

2. Numerical Method

This section presents the method of building an aircraft model suitable for determining the stability and control characteristics of fighter aircraft throughout the entire aircraft envelope. The first step in the method is to build a representative model of the complete aircraft of interest (including stores, control surfaces, inner loop control laws, aeroelastic effects, etc.). Next, simulations are performed of maneuvers designed to excite the relevant flow physics that will be encountered during actual missions in all three axes: roll, pitch, and yaw. These simulations are termed “computational maneuvers,” since they may be unreasonable to fly due to actual aircraft or pilot limits. A mathematical model is then built of the aircraft response using system identification/parameter estimation and tested by comparing CFD simulations against model predictions of conditions expected to be encountered in flight. Finally, predictions of all flight test points are made using the model before flight tests are conducted to determine the expected behavior of the actual aircraft. The following subsections describe the individual elements of the flow solver and system identification method necessary for the process.

Flow Solver: Cobalt

Computations were performed using the commercial flow solver *Cobalt*. *Cobalt* is a cell-centered, finite volume CFD code. It solves the unsteady, three-dimensional, compressible Reynolds Averaged Navier-Stokes (RANS) equations on hybrid unstructured grids. Its foundation is based on Godunov’s first-order accurate, exact Riemann

solver. Second-order spatial accuracy is obtained through a Least-Squares Reconstruction. A Newton sub-iteration method is used in the solution of the system of equations to improve time accuracy of the point-implicit method. Strang *et al* [3] validated the numerical method on a number of problems, including the Spalart-Allmaras model, which forms the core for the Detached Eddy Simulation model available in *Cobalt*. Tomaro *et al* [4] converted the code from explicit to implicit, enabling CFL numbers as high as 10^6 . Grismer *et al* [5] parallelized the code, yielding linear speed-up on as many as 2,800 processors. The parallel METIS (PARMETIS) domain decomposition library of Karypis *et al* [6] is also incorporated into *Cobalt*. Recent capabilities include rigid-body and 6 DOF motion, equilibrium air physics, Delayed DES [7] and overset grids in release *Cobalt V4.0*. An emerging capability still under development and testing in *Cobalt V5.0+* is moving control surfaces using overset grids. A coupled aeroelastic simulation capability is also being developed.

System Identification Analysis

System identification (SID) is the process of constructing a mathematical model from input and output data for a system under testing and characterizing the system uncertainties and measurement noises [8]. The mathematical model structure can take various forms depending upon the intended use. SID is usually applied to WT and FT data to obtain accurate and comprehensive mathematical models of aircraft aerodynamics for aircraft flight simulation, control system design and evaluation, and dynamic analysis. A comprehensive review of SID applied to aircraft can be found in Morelli and Klein [9,10] and Jategaonkar [11,12]. Aircraft system identification can be used in cooperative approaches with CFD to take advantage of the strength of both approaches or having one approach fill in the gaps where the other cannot be used [9]. The wide range of SID tools that have been developed for aircraft system identification can easily be used to analyze CFD data computed for aircraft in prescribed motion. Here we follow two techniques, the first being the global nonlinear parameter modeling technique proposed by Morelli [13] to describe the functional dependence between the motion and the computed aerodynamic response in terms of force and moment coefficients. The goal is to find a model which has adequate complexity to capture the nonlinearities while keeping the number of terms in the model low. The latter requirement improves the ability to identify model parameters, resulting in a more accurate model with good predictive capabilities. The second technique uses a radial basis function network (RBF), a form of artificial neural network that uses radial basis functions as activation functions. The network is based on the same inputs described in Morelli's approach and is a "universal approximator" on the compact dataset generated using CFD. RBFs have excellent nonlinear approximation properties which is why they are being investigated. Currently the RBF is trained via gradient descent training of the linear weights on the activation functions. The modeling efforts of both techniques are global because the independent variables ($\alpha, \dot{\alpha}, \beta$, etc.) are varied over a large range. Globally valid analytical models and their associated smooth gradients are useful for optimization, robust nonlinear control design, and global nonlinear stability and control analysis.

System Identification Analysis: Motivation

The ability to populate aerodynamic databases of new store configurations with SID models that capture full-scale static and dynamic aerodynamics, particularly when flight test and/or wind tunnel test resources are scarce, is highly desired to rapidly deliver new capability at reduced risk and cost. New CFD methods combined with HPC resources enables S&C engineers to begin investigating the plausibility of such an idea. The ultimate desire is to generate efficient yet accurate nonlinear aerodynamic models capable of predicting force and moment coefficients for both conventional static analysis and during the performance of traditional aircraft flight test maneuvers such as pitch doublets, yaw-roll doublets, sideslips, wind-up turns, rolls and high- α maneuvers. The goal is not to replace flight tests or wind tunnel tests, but rather to mitigate risk, improve S&C's predictive capability, improve test planning, and optimize available resources as efficiently as possible.

System Identification Analysis: Method

Time-accurate, dynamic, computational training maneuvers [2] are generated using a combination of chirp (sinusoid with varying frequency and varying amplitude) and/or stair-step signals to excite a range of aerodynamics during the maneuver. The resulting input angles, rates and output loads history (the training data)

are then modeled using the SIDPAC software [14] and/or RBF network. These models allow aerodynamic coefficient data to be extracted for comparison against known values. The training maneuver incorporates multiple rotations and/or translations to ensure proper "regressor space" coverage. The "regressor space" is the range of angles and rates that an aircraft would typically see during normal flight. Failure to properly train the model with adequate point density throughout the "regressor space" has been shown to result in poor model predictions. Input parameters to the models are chosen to enhance the model's "fit" to the training data [15].

3. Validation Data

This section describes the data used for validating results from static and dynamic CFD simulations of the USAF A-10C Thunderbolt II, F-16C Falcon, and F-22 Raptor.

A-10C Wind Tunnel Data

Wind tunnel tests were conducted at the Arnold Engineering Development Center's closed-loop, continuous flow, variable density 4T/16T WT in 1978-80. Using 1/20th scale models of the A-10 aircraft, with pylons, stores, and store racks, S&C data was obtained at Mach numbers from 0.3 to 0.75 at a total pressure from 800 to 2000 psfa. The angle-of-attack ranged between -4 and 20 degrees and the sideslip angle ranged from -10 to 10. The A-10 references below to WT data are with respect to these results.

F-16C Wind Tunnel Data

Wind tunnel tests were conducted at the Arnold Engineering Development Center's closed-loop, continuous flow, variable density 4T WT in 2007. Using 1/20th scale models of the F-16C Block 40 aircraft, AGM-154 JSOW, GBU-39 SDB, BRU-61 rack, suspension equipment, tanks, missiles and pods, S&C data was obtained at Mach numbers from 0.6 to 2.0 at a total pressure of 1200 psfa. The angle-of-attack ranged between -6 and 26 degrees and the sideslip angle ranged from -16 to 16 degrees. Using the move-pause technique, data was recorded at specified angles while tunnel conditions were held constant. The F-16 references below to WT data are with respect to these results.

F-16C Lockheed Martin Performance Data

F-16C Block 40 performance data came from two sources. Data that includes scheduled leading edge flaps (LEF) is based on flight test (FT) results. Data with fixed LEFs is based on 1/9th scale model WT results. Both sets of data have had engine effects removed and are corrected to full scale conditions at their corresponding Mach and altitude. The data is also corrected with Block 40 deltas from earlier F-16 variants.

F-16C ATLAS and F-22 ATLAS Programs

Lockheed Martin's Aircraft Trim, Linearization and Simulation (ATLAS) program is a generalized, 6-DOF, nonlinear, non real-time simulation. It is a non real-time version of Lockheed Martin's flying qualities simulator. The aerodynamic database for ATLAS is based on WT test data and includes all flight test corrections.

F-22 AVTEST

Lockheed Martin's AVTEST is a frontend used to extract aerodynamic data for the F-22. The aerodynamic database in AVTEST was developed from wind tunnel and flight tests and includes all relevant corrections. AVTEST differs from ATLAS in that specific deltas can be independently selected. Such options include the ability to extract pure wind tunnel data up to fully flight test corrected data with and without propulsion effects as well as specifying individual control surface deflections, engine settings, rigid body versus flex effects, and store configurations. This flexibility allows extraction of total or partial aerodynamic coefficients for accurate, 1:1 comparison to CFD results for both static and dynamic analysis.

4. Results

The discussion below encompasses studies of USAF fighter aircraft with and without stores that include A-10C, F-16C, and F-22 using the CFD solver *Cobalt*. Multi-axis computational training maneuvers [2], prescribed motion flight test maneuvers using flight test data, and control surface deflection simulations were investigated. For the A-10, analysis has been performed on clean aircraft and aircraft with a centerline fuel tank. Static, time-accurate simulations investigating longitudinal and lateral-directional stability and prescribed motion, computational training maneuvers have been performed in CFD. For the F-16, analysis has been performed on clean aircraft and aircraft with stores. CFD simulations of static, time-accurate simulations investigating longitudinal and lateral-directional static stability and prescribed motion, flight-test maneuvers with moving control surfaces have been performed. Results presented of the F-22 are in the clean configuration and with external fuel tanks. F-22 results include static, time-accurate simulations and prescribed motion, flight-test maneuvers investigating longitudinal and lateral-directional static and dynamic stability. Nonlinear, reduced-order, aerodynamic models have been generated using SID of CFD simulations. The SID models were tested against static and dynamic data. As detailed above, wind tunnel data, flight test data and Lockheed Martin aerodynamic data serve as validation data.

All simulations were run on DoD HPC systems. Static, time-accurate simulations were run on 128 to 512 cores, at a time step of 0.0004 seconds and with 3 - 5 Newton sub-iterations. Dynamic, time-accurate, prescribed motion, computational training maneuvers and flight-test maneuvers were run on 512 - 1,000+ cores at a time step of 0.0004 seconds and with 5 Newton sub-iterations. All grids are unstructured and were created with SolidMesh [16], a solid modeling and unstructured grid generation system, and the AFLR grid generator [17,18] (Mississippi State). Full-span grid sizes ranged from 13 million cells for a clean F-16C to 30+ million cells for a fully loaded aircraft with stores. All grids are unstructured mixed element grids containing tetrahedral and five and six sided pentahedral elements. An initial boundary layer spacing of $y^+ = 1$ was specified for all grids. Additionally, transparent surfaces were used in areas of interest to capture vortical flow and shedding.

F-16C Static Analysis: Clean Aircraft with Tip AIM-9s

Full-scale, static time-accurate analysis of an F-16C with tip AIM-9 missile, shown in **Figure 1**, was performed using *Cobalt*. Longitudinal results for an alpha sweep from 0 to 28 degrees angle of attack (AoA) at Mach 0.9 are shown in **Figure 2** with C_L , C_D , and C_m plotted from left to right. Lockheed Martin performance data for the same loading is shown for comparison. CFD results are a near perfect match for C_L and C_D at 0.9 Mach. Although moment curves do not fall completely within the set thresholds, they do show the correct trend and magnitude.

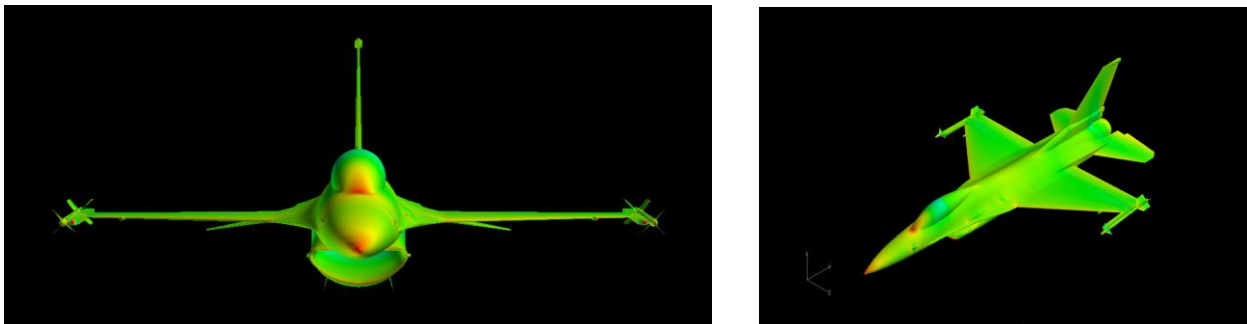


Figure 1. F-16C configured with tip AIM-9 missiles.

Due to restrictions on releasing technical data to the general public specified by the USAF and DoD, an alternate method of presenting results is implemented throughout this paper. In order to show the difference between CFD and validation data, whether it is Lockheed Martin performance data, wind tunnel data, or ATLAS/AVTEST data, results are plotted as percent error from the validation data as opposed to plotting the actual values of the data, except where necessary to more clearly illustrate the results. For example, the top left plot in **Figure 2** is a

conventional plot showing AoA as the independent variable along the X-axis and the C_L values for the different datasets as the dependent variables along the Y-axis. The lower left plot in **Figure 2** shows the alternative method implemented throughout the remainder of this paper by plotting AoA as the independent variable along the X-axis with C_L % error plotted along the Y-axis, resulting in a horizontal line with a Y-axis intercept of zero (denoted by the blue trace). Each C_L value obtained from CFD is then plotted on the Y-axis (denoted by the red and light blue, dotted traces respectively) against the corresponding X-axis AoA value as a percent error from the validation data value at that point. For a perfect match between the CFD and validation data, the CFD data should lie on top of the horizontal line with a constant slope of zero. Discrepancies in the CFD data against the validation data are illustrated as shifts above or below the horizontal line.

A downside to this approach is that the magnitude of the delta between CFD and validation data is unclear since there are no scale values along the X- or Y-axes. To bound the error, thresholds (denoted by the gray, dotted lines) are plotted and represent the percent error from the “truth” data that CFD results would ideally fall within to support S&C store certification activities. Where actual curve shapes are plotted with thresholds present, the threshold is computed by taking a $\pm 5\%$ difference from each validation data point $\pm 5\%$ of the maximum absolute value of the validation data. The threshold then does not reduce to zero with the validation data, providing a more tolerant threshold at lower values. The threshold is nominally set at 10% error for the alternate plot style.

It should be noted that these thresholds, relative to a validation dataset, represent what an idealized CFD solution would satisfy. They are not based on a single, specific test or a lengthy history of CFD implementation in the S&C community. Furthermore, consensus within the broader S&C community regarding what represents an 'acceptable' and 'unacceptable' CFD solution throughout the flight envelope has not been realized. Taken together, these thresholds merely represent a way to quantify the delta between a validation dataset and the respective CFD solution for discussion purposes. Although results may fall outside these thresholds, overall trends are useful in implementing engineering judgment.

Using the above methods, plots of C_L , C_D , and C_m are shown in **Figure 2** from left to right. Lockheed Martin performance data for the same loading are shown for comparison. The CFD results compare well with the validation data for forces and moments and are almost entirely within the threshold values set.

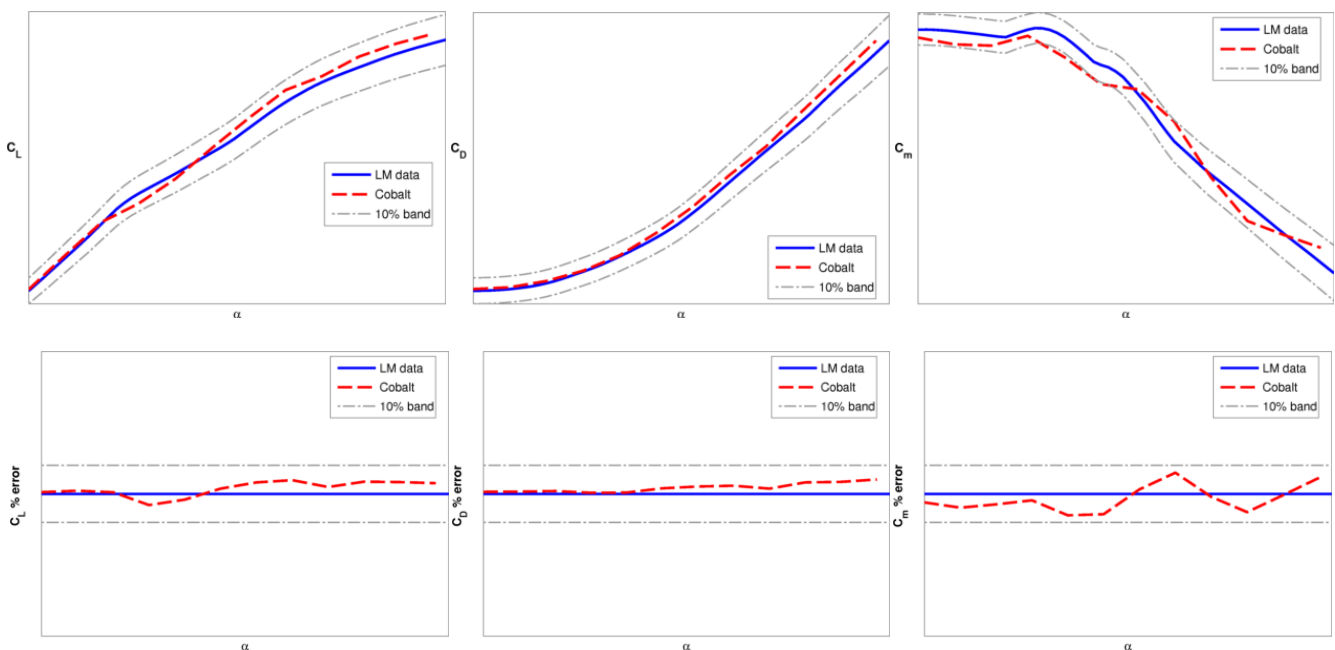


Figure 2. F-16C CFD (Cobalt, full-scale) with LEF = 0 degrees vs. LM Performance Data with LEF = 0 degrees for C_L , C_D and C_m , Mach 0.9.

A-10C Static SID Analysis: Clean

Full-scale, static time-accurate analysis of an A-10C in the clean configuration was performed using *Cobalt*. **Figure 3** shows the A-10C grid in clean configuration colored by pressure. A dynamic computational training maneuver was also performed in CFD to examine the effectiveness of a new maneuver design in more accurately capturing the static stability characteristics of an aircraft using a single dynamic CFD maneuver. The new maneuver design incorporates a “stair-step” approach during which the aircraft is “stepped” through the desired ranges of angle of attack and sideslip.

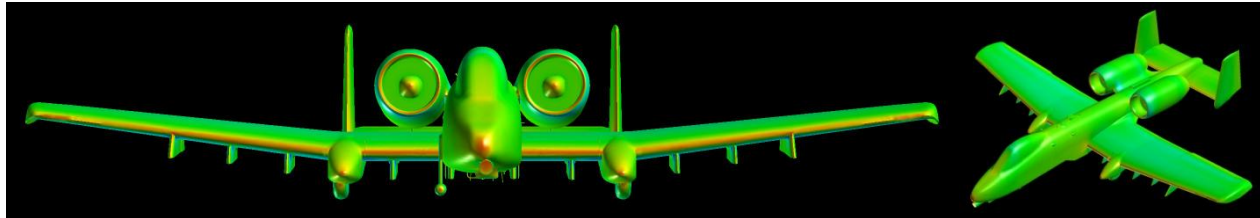


Figure 3. A-10C in clean configuration

The mesh simulated had 24.7 million cells and the simulation required 18.5 seconds per time step on 512 cores of ERDC DSRC’s system Diamond for the computational training maneuver and approximately 24.2 seconds per time step on 256 cores of ERDC DSRC’s system Diamond for the static runs. For the maneuver shown in **Figure 4**, 125 iterations, each with 5 sub iterations, are calculated at each “step.” This increased number of iterations at each “step” allows for greater confidence in the accuracy of the static data extracted from the dynamic maneuver.

Longitudinal results with multivariate polynomial (MVP) and radial basis function (RBF) SID model predictions developed from the new “stair-step” training maneuver for an alpha sweep from 0 to 20 degrees angle of attack (AoA) at Mach 0.3 are shown in **Figure 5** with C_L , C_D , and C_m plotted from left to right. Lateral-directional results for a beta sweep from -12 to 12 degrees angle of sideslip (β) at 0 degrees AoA and Mach 0.3 are shown in **Figure 6** with C_Y , C_l , and C_n plotted from left to right. Wind tunnel test data for the same loading is shown for comparison. CFD results match well for C_Y and C_n , but an offset is seen for the rest of the force and moment coefficients in **Figure 5** and **Figure 6**. The cause of the offset is being investigated. It is worth noting that the SID models predict the CFD static data well for all six coefficients, and, once the cause of the offset is determined, the SID models will be corrected if necessary.

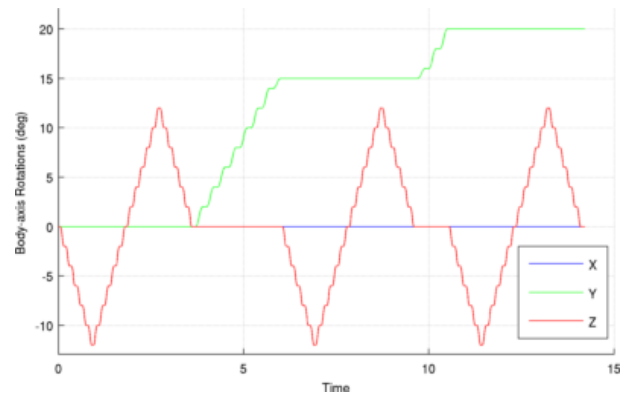


Figure 4. New "stair-step" dynamic CFD training maneuver.

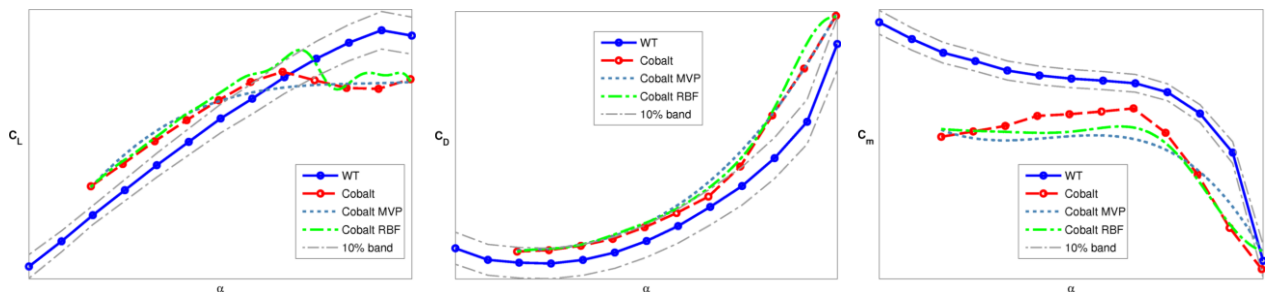


Figure 5. C_L , C_D , and C_m comparison for the A-10C at Mach 0.3 and $\beta = 0$ degrees.

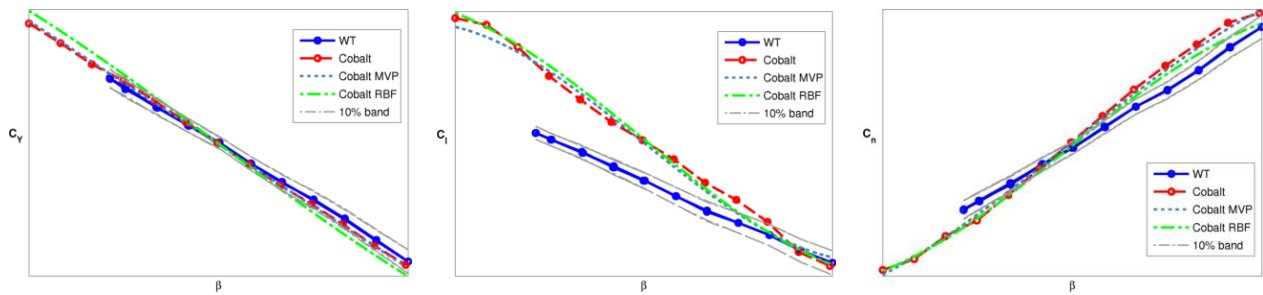


Figure 6. C_Y , C_l , and C_n comparison for the A-10C at Mach 0.3 and AoA = 0 degrees.

A-10C Static SID Analysis: Centerline Fuel Tank

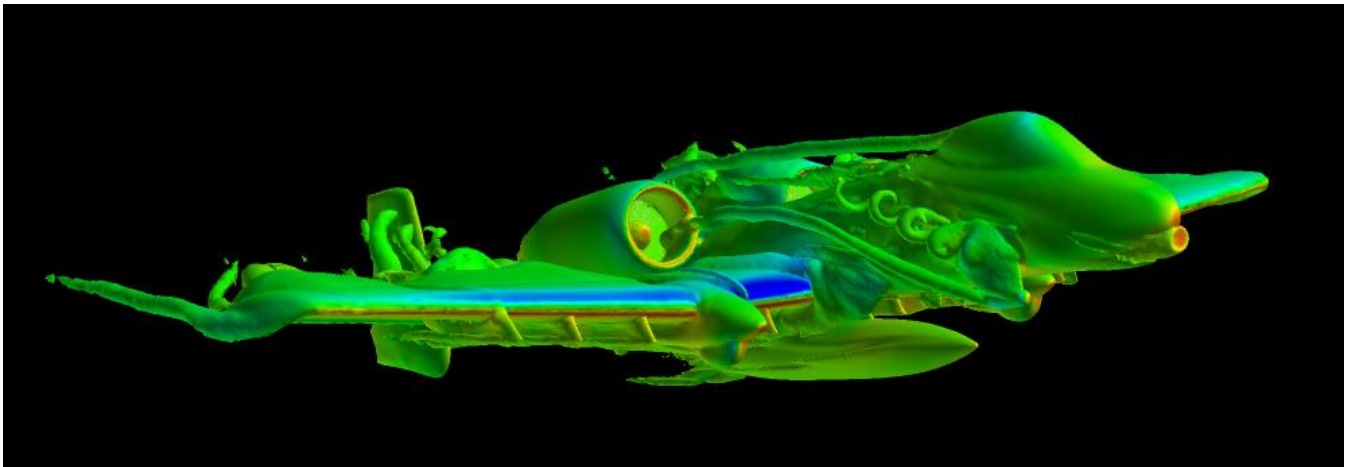


Figure 7. A-10C with fuel tank at Mach 0.3.

Full-scale, static, time-accurate analysis of the A-10C configured with a 600-gallon centerline fuel tank was performed to investigate the effects of the fuel tank on A-10C static stability and control. **Figure 7** shows the A-10C with isosurfaces of vorticity colored by pressure at Mach 0.3. As with the clean configuration already discussed, a “stair-step” dynamic computational training maneuver was also performed in CFD. The mesh simulated had 19.6 million cells and the simulation required 12.4 seconds per time step on 512 cores of ERDC DSRC’s system Garnet for the computational training maneuver and approximately 16 seconds per time step on 256 cores of ERDC DSRC’s system Garnet for the static runs. Static results from the *Cobalt* CFD solver compared with multivariate polynomial (MVP) SID model predictions developed from the new “stair-step” training maneuver are shown in **Figure 8**. Results for C_Y , C_l , and C_n are shown left to right. No wind tunnel or flight test data was available for comparison at the time of this writing. For the SID model, the training maneuver covered a regressor space of 0 to 10 degrees angle of attack and -8 to 8 degrees of sideslip. Results show a good match between the static simulations and the model predictions out to the limits of the covered regressor space. Given previous difficulty in obtaining accurate lateral-directional models from training maneuver data, the results in **Figure 8** are promising.

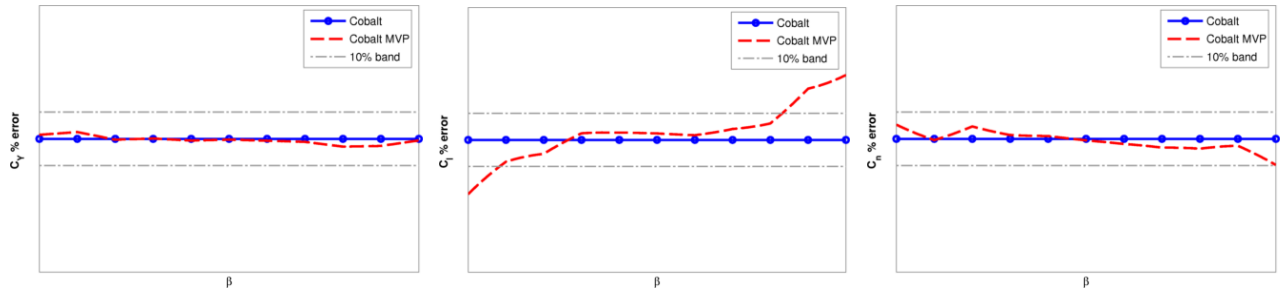


Figure 8. C_Y , C_l , and C_n comparison for the A-10C at Mach 0.3 and AoA = 0 degrees.

F-16C Static SID Analysis: AGM-154 JSOW and GBU-39 SDB

Exploring the idea of early discovery of complex aerodynamic phenomena that are typically not discovered until flight test, SID of CFD and time accurate static analysis were conducted near Mach 1.2 and 20,000 feet to determine if the same instabilities detected in wind tunnel test and flight test could be reproduced. **Figure 9** depicts the F-16 JSOW configuration and one instant from the training maneuver simulation depicting isosurfaces of vorticity colored by pressure. The mesh simulated had 24.5 million cells and the simulations required approximately 20 seconds per time step on 256 cores of AFRL's system Raptor for the static runs. An example of the resulting model equations obtained from the SID analysis [19] is shown in **Equation 1** where the model terms are listed in order of most influential to least influential. Predictions from this yawing moment coefficient model result in a goodness of fit of 98.83% when compared with the training data.

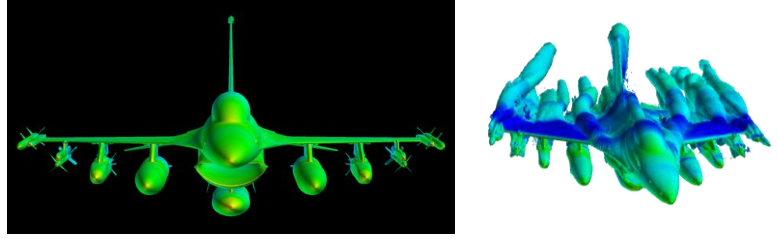


Figure 9. F-16 JSOW on Parent Pylon configuration (left) and CFD training maneuver flow simulation (right).

$$C_n(\alpha, \dot{\alpha}, \beta, \dot{\beta}, r, M) = C_1\beta + C_2r + C_3\beta^2r + C_4\dot{\alpha}\beta M + C_5\alpha M^2 + C_6\beta M^2 + C_7\beta M + C_8rM + C_9\beta^3 + C_{10}\dot{\alpha}\beta\dot{\beta} + C_{11}\dot{\alpha}\beta r + C_{12}\alpha\beta^2 + C_{13}\alpha\beta + C_{14}\alpha\beta M + C_{15}\alpha\dot{\alpha}\beta + C_{16}\beta^2\dot{\beta} + C_{17}\dot{\alpha}\beta^2 + C_{18}\dot{\beta} + C_{19}\dot{\alpha}r^2 \quad (1)$$

The ultimate desire is to generate efficient yet accurate nonlinear aerodynamic models capable of predicting force and moment coefficients for both conventional static analysis and during the performance of traditional aircraft flight test maneuvers such as pitch doublets, yaw-roll doublets, sideslips, wind-up turns, and rolls. **Figure 10** depicts plots of C_Y , C_l and C_n versus angle of sideslip for a beta sweep at Mach 1.2 and 20,000 feet from -12 to 12 degrees of sideslip for the JSOW on Parent Pylon configuration compared with SDB wind tunnel data. Wind tunnel test results [20] confirmed the SDB on BRU-61 is analogous to the JSOW from an S&C perspective, thus wind tunnel test results from either SDB or JSOW configurations are used for comparison with CFD data when finding the closest match to the CFD grid configuration. In **Figure 10**, wind tunnel data of a full SDB configuration (blue, SDB 2683) is plotted against a clean configuration (only tip AIM-120 missiles, red, SDB 2538), JSOW on Parent Pylon CFD results, and SID of CFD results. **Figure 11** depicts plots of C_Y , C_l and C_n versus angle of sideslip for a beta sweep at Mach 1.1 and 20,000 feet from -12 to 12 degrees of sideslip for the JSOW on BRU-57 configuration. In **Figure 11**, JSOW on BRU-57 wind tunnel data (blue, WT2184) is compared with a clean configuration (only tip AIM-9 missiles, red, WT2499) and JSOW on BRU-57 CFD results. The CFD and SID of CFD results are expected to follow the blue curves. A reduction in directional (weathercock) stability, C_n , is apparent when comparing SDB 2683 vs. SDB 2538 and WT 2184 vs. WT 2499. An increase in dihedral effect seen in the steepening of the C_l curve is apparent when comparing the same WT result pairs. **Figure 10** and **Figure 11** illustrate CFD's and SID of CFD's ability to predict these changes in static stability, which indicate the possibility of a high frequency Dutch roll and uncommanded yaw-roll oscillation. These phenomena associated with large store configurations on the F-16 are known and well documented.

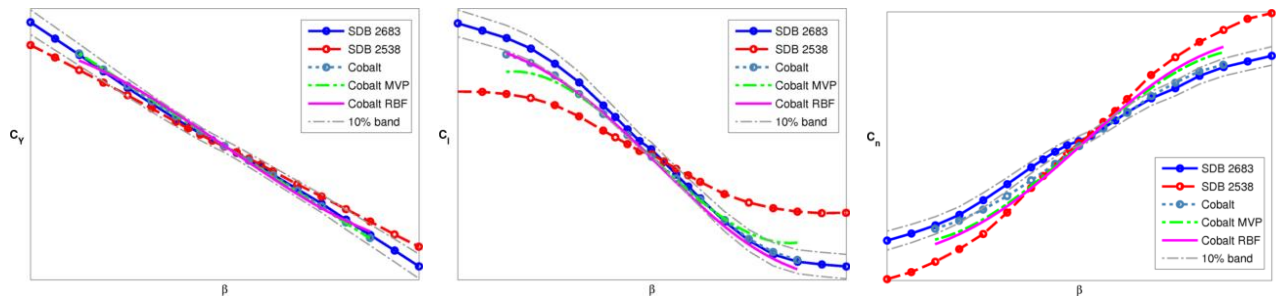


Figure 10. Cobalt CFD and SID of CFD of C_Y , C_l and C_n versus WT data for JSOW on Parent Pylon for a beta sweep at Mach 1.2 and 20,000 feet.

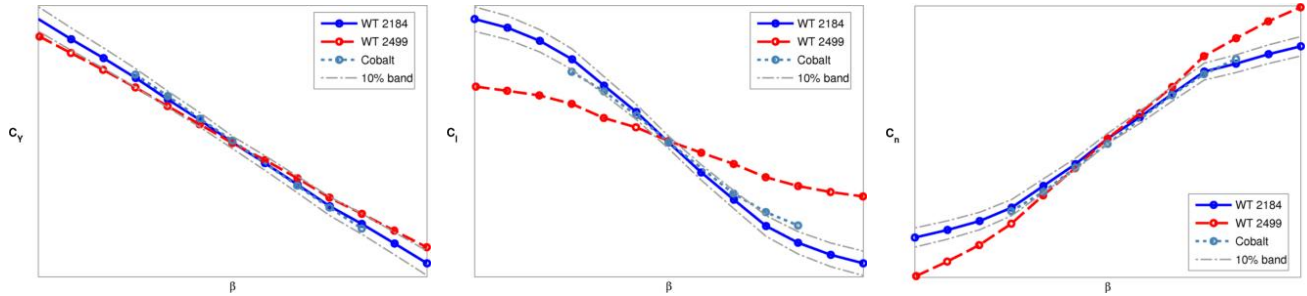


Figure 11. Cobalt CFD of C_Y , C_l and C_n versus WT data for JSOW on BRU for a beta sweep at Mach 1.1 and 20,000 feet.

F-22 Static Analysis: External Fuel Tanks

Full-scale, static, time-accurate analysis of the F-22 configured with two external fuel tanks was conducted. Shown in **Figure 12** is a static, time-accurate simulation depicting isosurfaces of vorticity colored by pressure at Mach 0.95. The mesh simulated had 24.3 million cells and the simulation required approximately 20.3 seconds per time step on 256 cores of ERDC DSRC's system Garnet. Lockheed Martin AVTEST aerodynamic data serves as validation data for external tank configurations. A comparison between AVTEST data for clean and with tank configurations is shown in **Figure 13** to give a sense of the expected difference between clean and with tank configurations. AVTEST data for the clean configuration is compared with CFD data in **Figure 14** while the tank configuration data is compared in **Figure 15**. Longitudinal forces and moments match AVTEST validation data well for both the clean and with tank configurations. CFD results have been incorporated into the LM ATLAS software for external fuel tank configurations and show very similar maneuver response when compared to ATLAS time histories of the same configuration.

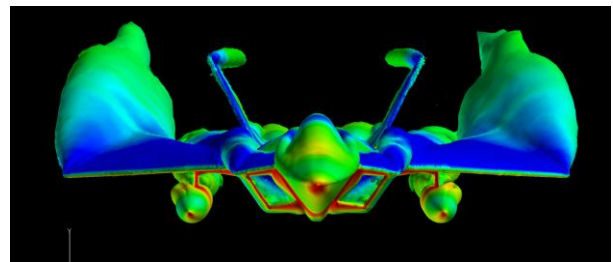


Figure 12. F-22 static, time-accurate simulation at Mach 0.95.

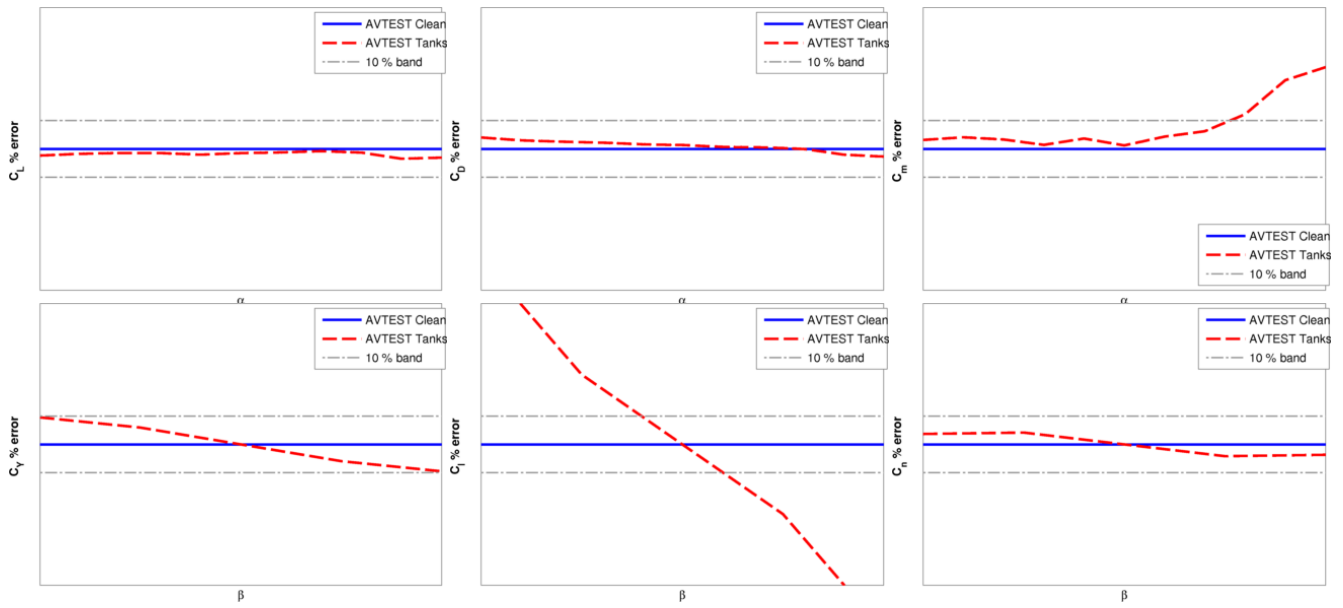


Figure 13. LM AVTEST Clean vs. with Tanks Data for C_L , C_D , C_m , C_Y , C_I , and C_n , Mach 0.95.

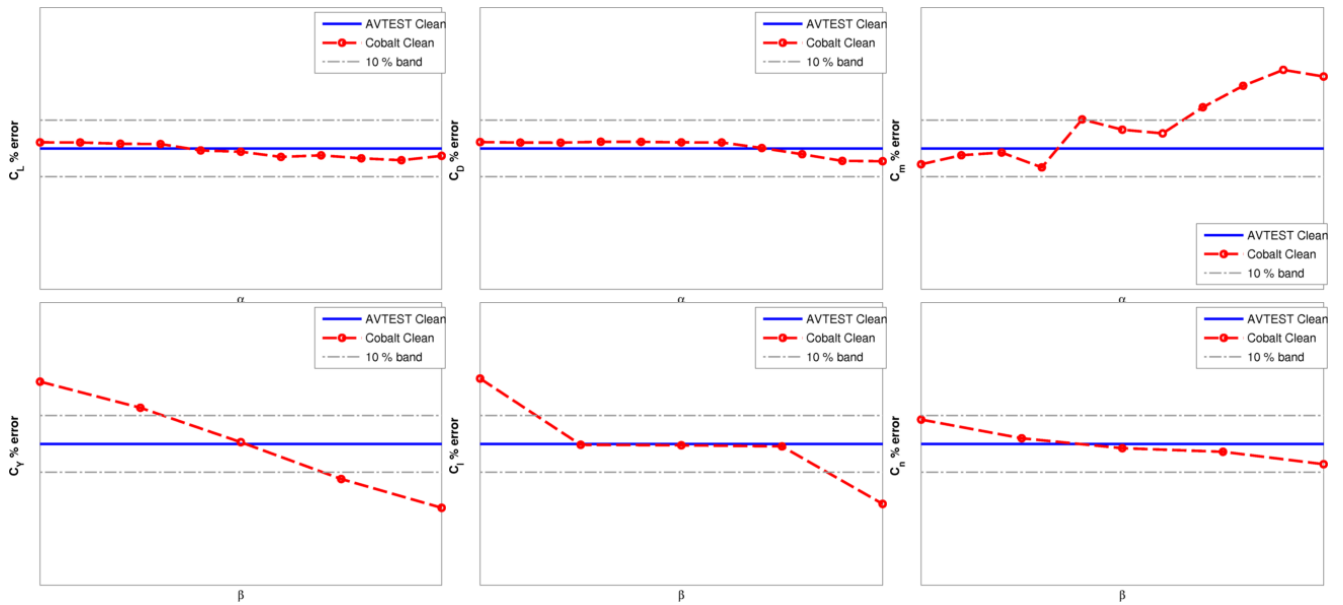


Figure 14. F-22 CFD (Cobalt, full-scale) vs. LM AVTEST Data Clean for C_L , C_D , C_m , C_Y , C_I , and C_n , Mach 0.95.

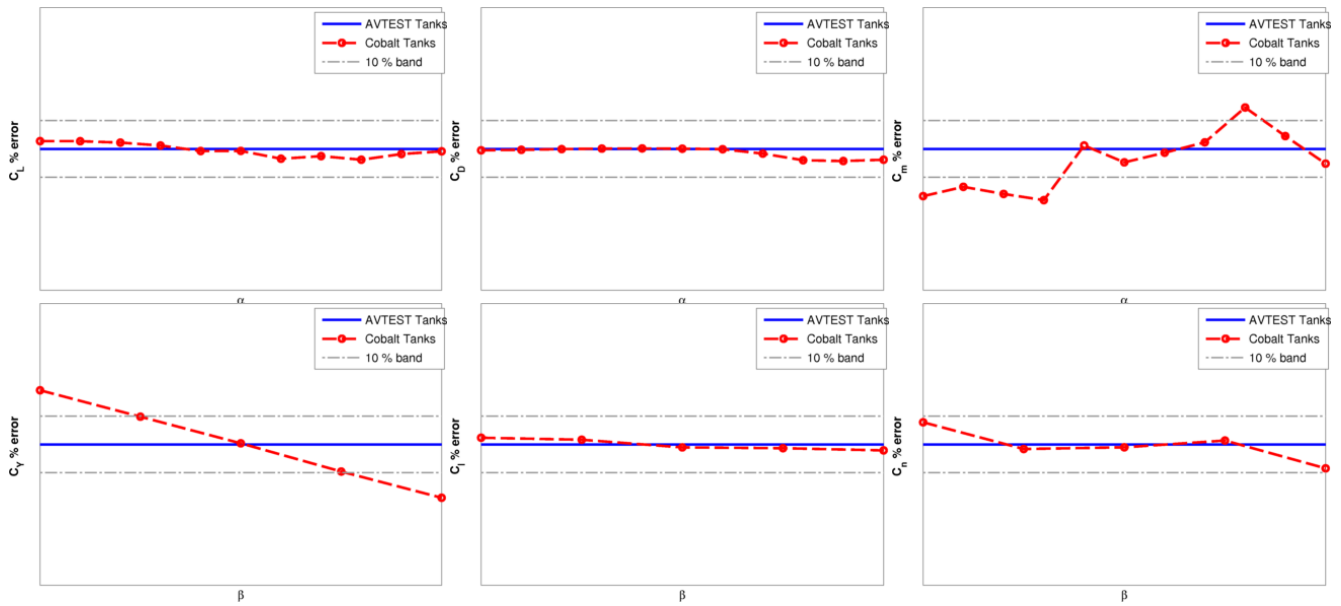


Figure 15. F-22 CFD (*Cobalt*, full-scale) vs. LM AVTEST Data with Tanks for C_L , C_D , C_m , C_Y , C_l , and C_n , Mach 0.95.

F-22 Dynamic Analysis: J-Turn

In the absence of digital flight test data available at the time, an F-22 performing a Herbst or J-Turn maneuver at Mach 0.6 was simulated using Lockheed Martin's F-22 ATLAS program. The Herbst maneuver is a high angle of attack maneuver that requires thrust vectoring and other features unique to the F-22. The maneuver response output data from the ATLAS simulation was used to generate a prescribed motion input file. This motion file was then used to perform the maneuver in CFD using *Cobalt*. The mesh depicted in **Figure 17** had 16.3 million cells and the simulation required 3.4 seconds per time step on 1024 cores of MHPCC's machine Mana. The maneuver simulation was for 34 seconds of physical time with a time step of 0.0004 seconds requiring 84,500 iterations. The wall-clock time for performing the simulation was approximately 80 hours.

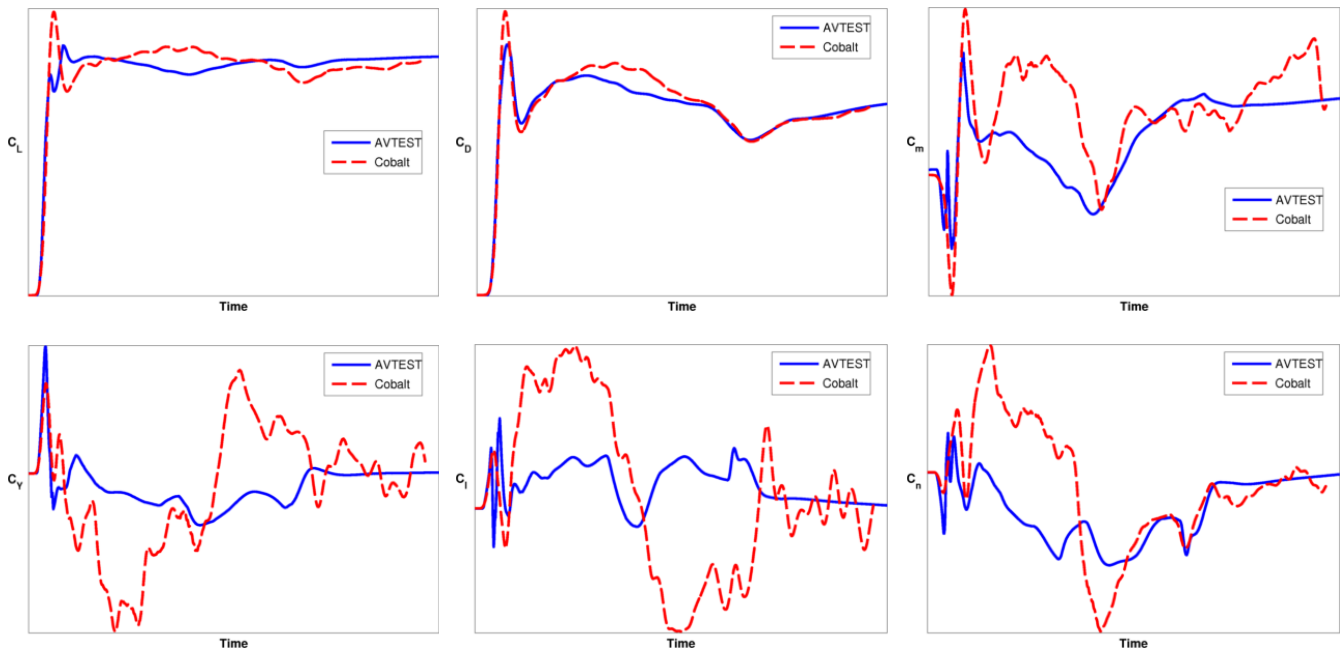


Figure 16. F-22 CFD (*Cobalt*; full-scale) vs. LM AVTEST Data for C_L , C_D , C_m , C_Y , C_l , and C_n during a J-Turn, Mach 0.6.

Output from the ATLAS simulation was also used with Lockheed Martin's AVTEST aerodynamic database. Using the features within AVTEST, time histories were generated of the aerodynamic data, including dynamic effects such as alpha-dot and q, over the course of the maneuver without flexibility effects, the effects of control surface movement or thrust. This enabled a genuine, full-scale, 1:1 comparison between CFD and Lockheed validation data for the same maneuver. **Figure 16** shows the Lockheed AVTEST time history in blue (solid line). The red, dashed curve depicts the maneuver performed in CFD using *Cobalt*. As seen in **Figure 16**, while the magnitude of the forces and moments are close, the agreement between CFD and AVTEST is less than in previous runs. It is hypothesized, that since the maneuver occurs almost entirely within the post stall region of the flight envelope, the solution is harder to determine. It is possible, that with additional grid and solver refinements a closer match could be achieved.

The frames in **Figure 17** show six different time steps during the simulation of the J-Turn turn maneuver. As the aircraft increases angle of attack, resulting in increased lift and drag, the vortices above the inlets at the wing's leading edge and off the forward fuselage become more pronounced.

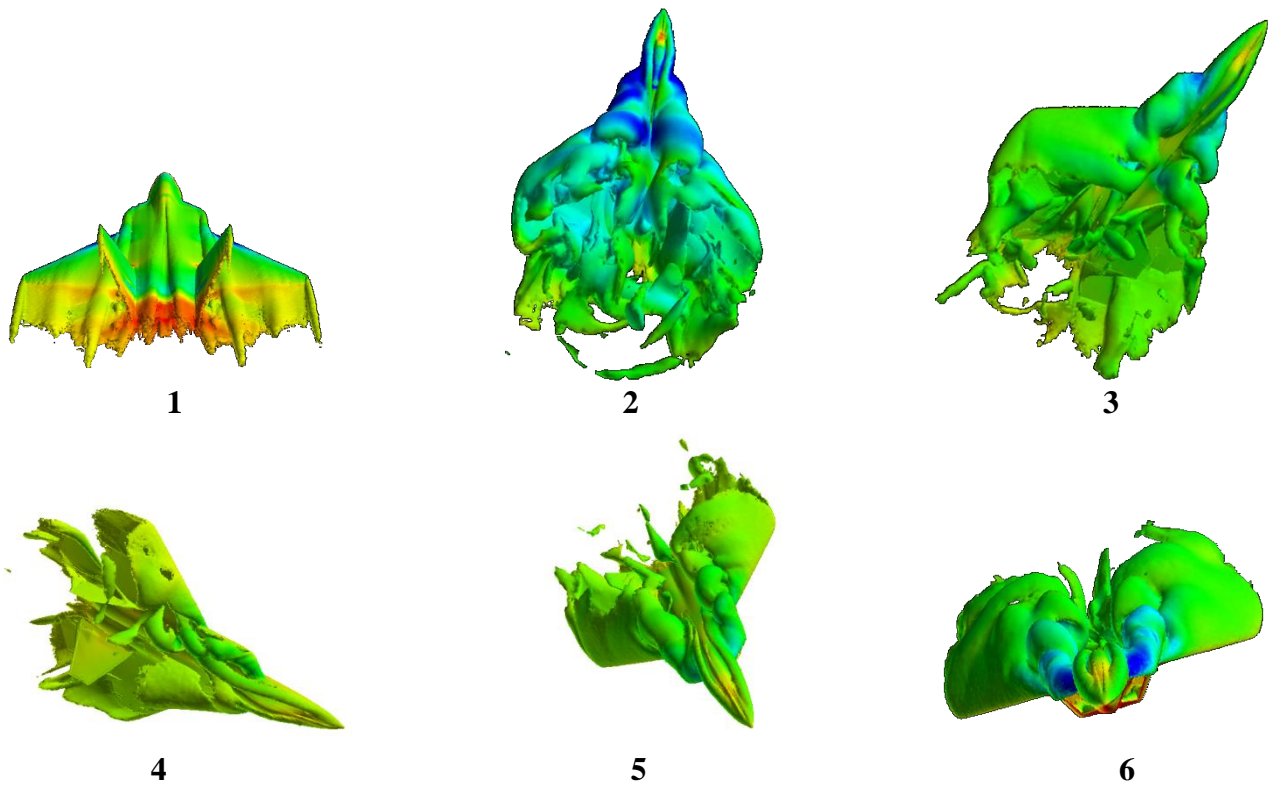


Figure 17. Selected frames from F-22 J-Turn simulation in CFD (*Cobalt*) at Mach 0.6.

F-16 Moving Control Surface Analysis: Pitch Doublet

Modeling moving control surfaces on a full-scale aircraft is the next step in capability development. Two simulations for the same maneuver were conducted. Full-scale, dynamic, time-accurate analysis of the F-16 in the clean aircraft configuration, with moving horizontal tails, and with moving horizontal tails and moving leading edge flaps (LEF) is accomplished using *Cobalt* and the overset grid method. The aircraft and control surfaces motions are accomplished by reading in time histories computed using ATLAS and forcing the aircraft and control surfaces through a prescribed motion. **Figure 18** depicts the F-16 horizontal tail and LEFs at different instances from the pitch doublet simulation. The horizontal tail is shown at center, maximum leading edge down, and maximum leading edge up deflections and the LEF is shown at the starting in-flight condition and maximum leading edge down deflection. Color contours depict pressure variations over the surface during the maneuver.

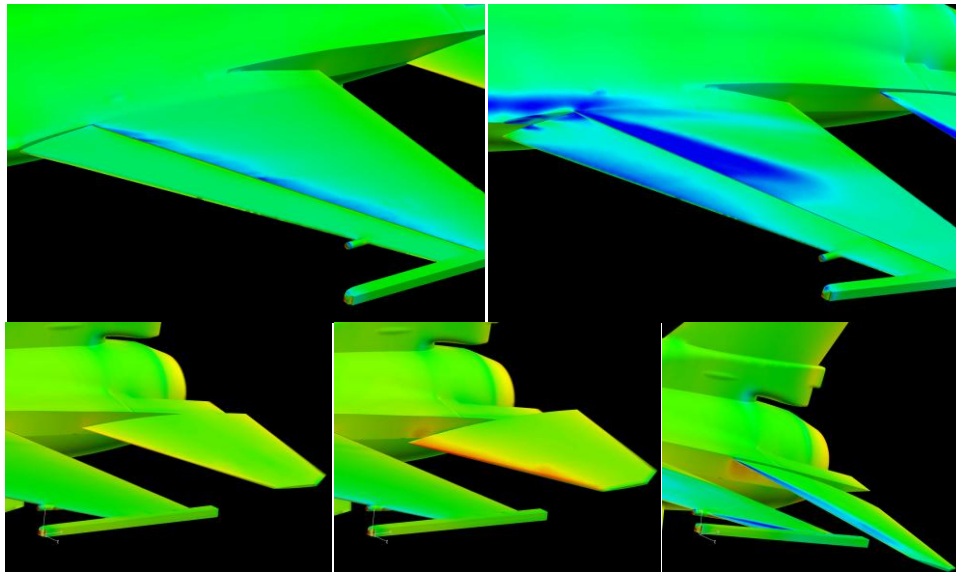


Figure 18. Overset Grid of Clean F-16 with moving horizontal tails and LEFs at Mach 0.6 and 10,000 feet.

Longitudinal results for C_L , C_D and C_m are shown left to right in **Figure 19**. ATLAS aerodynamic data serves as validation data. Overall, forces and moments match well for both maneuvers in that the trend and magnitude are similar throughout the entire maneuver. It can be seen in the plot of C_L that the grid with moving LEFs (blue curve) does not predict validation data (red curve) as well as the grid with only HTs (black curve) modeled. This reduced lift may be an artifact of how the LEFs were modeled. Because the grid with moving LEFs has a gap where the control surface hinge line is modeled there is an expected loss of high pressure bleeding up to the low pressure side of the wing. This gap is not present on actual aircraft. The HT&LEF curve for the pitching moment coefficient shows a much better fit to the validation data than the curve with just HTs modeled. This was expected due to the large influence LEFs have on pitching moment. In this and previous papers, moments are often not predicted as well as the forces. These results are promising and the other moments are expected to improve as control surfaces come online.

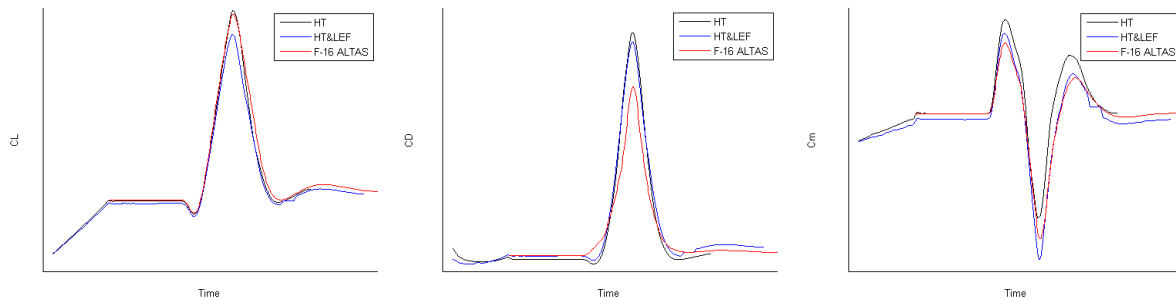


Figure 19. F-16 Pitch Doublet CFD simulation with moving horizontal tails and LEFs at Mach 0.6 and 10,000 feet.

The overset grid generated to model the horizontal tail control surfaces increased the number of grid cells by 11.68 million over the rigid body grid. To model all control surfaces, the clean grid is increased by approximately 31.10 million cells. The amount of time per iteration utilizing 512 processors and the DoD HPC machine Garnet was approximately six minutes per iteration for the grid with all moving control surfaces modeled. The approximate time per iteration for a dynamic, time-accurate simulation without moving control surfaces and using 512 processors is approximately 10-15 seconds per iteration on Garnet. This increase in required time will need to be addressed in the future if CFD is to be used as a M&S tool for aircraft-store certification activities.

F-16 Overset Grid: Moving Control Surfaces

An unstructured overset method was used to simulate moving control surfaces in Cobalt. Gaps were introduced between the wing and the control surface to allow the surfaces to rotate about the hinge line without intersecting. **Figure 20** below left, is a snapshot of the F-16 grid with control surfaces cutout. It can be seen that much of the increase in grid size, an increase of 31.10 million cells, is due to the dense point spacing around the surface gaps; the area that looks like shading around the control surfaces. To create gaps between the fuselage and the Leading Edge Flaps (LEFs), flaperons, and rudder part of the control surface was removed. On the long edges (hinge line) of these control surfaces, material was removed from the non moving aircraft surface. To allow rotation, the inner edge of the control surface was rounded and a matching offset surface created in the wings and vertical stabilizer. As the horizontal tails are all moving, a gap was created by translating them away from the body. A gap distance of 0.25” was utilized to allow enough space to avoid problems with grid reconstruction during simulated movement. A downside to gap cutting is that material is removed from the model and air is free to flow through the gaps. This is not representative of actual aircraft design, and the effects have yet to be determined.

Figure 20 below right, shows the inboard intersection of the wing (green), LEF (magenta), and body (orange) on the F-16 in the non deflected position.

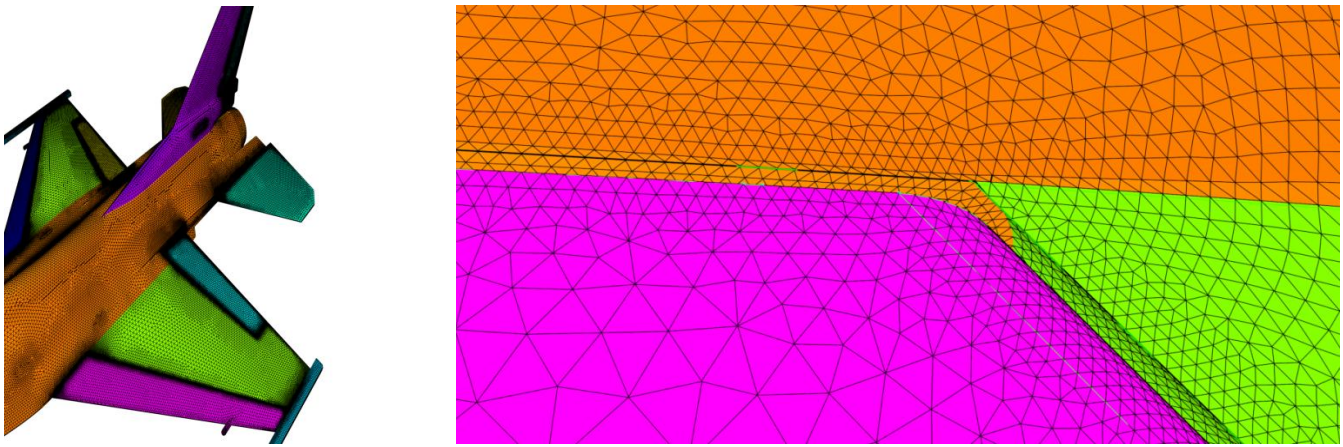


Figure 20. F-16 grid with control surfaces cutout (left) and the Inboard intersection of the wing (green), LEF (Magenta), and body (orange) (right).

5. Current Work

Although prescribed motion, moving control surface maneuvers are a great step toward imitating real-world flight test maneuvers in a computational environment, no simulation, or virtualization, of flight test maneuvers could be complete without the capability of the simulation to react to and act upon the computational environment. Thus the current work focuses not only on refining the mechanism to successfully move the aircraft and control surfaces using prescribed motion, but also on using feedback control and 6-DoF simulation to allow both the simulated aircraft and the virtual environment to react to and act upon one another.

Cobalt has built within it the capability to accept external feedback control to manipulate both the grid motions and the surface boundary conditions (BC) during computation of the CFD solution. This ability allows the user to alter, during the CFD simulation, both the grid positions for deflecting control surfaces using motion control and, for instance, the thrust setting from the engine exit using BC control. Also, 6-DoF code can be coupled with the feedback control code to have the aircraft react realistically to the control surface motion and boundary condition inputs. **Figure 21** outlines the process of using external feedback control with *Cobalt* for computing a CFD solution.

External feedback control is handled via MATLAB using a MATLAB interface built into *Cobalt*. Four files are required from the user to handle the interaction of the feedback control interface between *Cobalt* and MATLAB. The four files are as follows:

1. Control file – sets up the interface for passing information between *Cobalt* and MATLAB; called only once at the beginning of the simulation.
2. Init file – initializes the feedback control routines and any necessary parameters and variables; called only once at the beginning of the simulation.
3. Iterate file – the main feedback control file; all motion, BC, and 6-DoF algorithms are contained within or called from this file; called every iteration.
4. Wrapup file – allows for calling any finalization or cleanup routines; called only once at the end of the simulation.

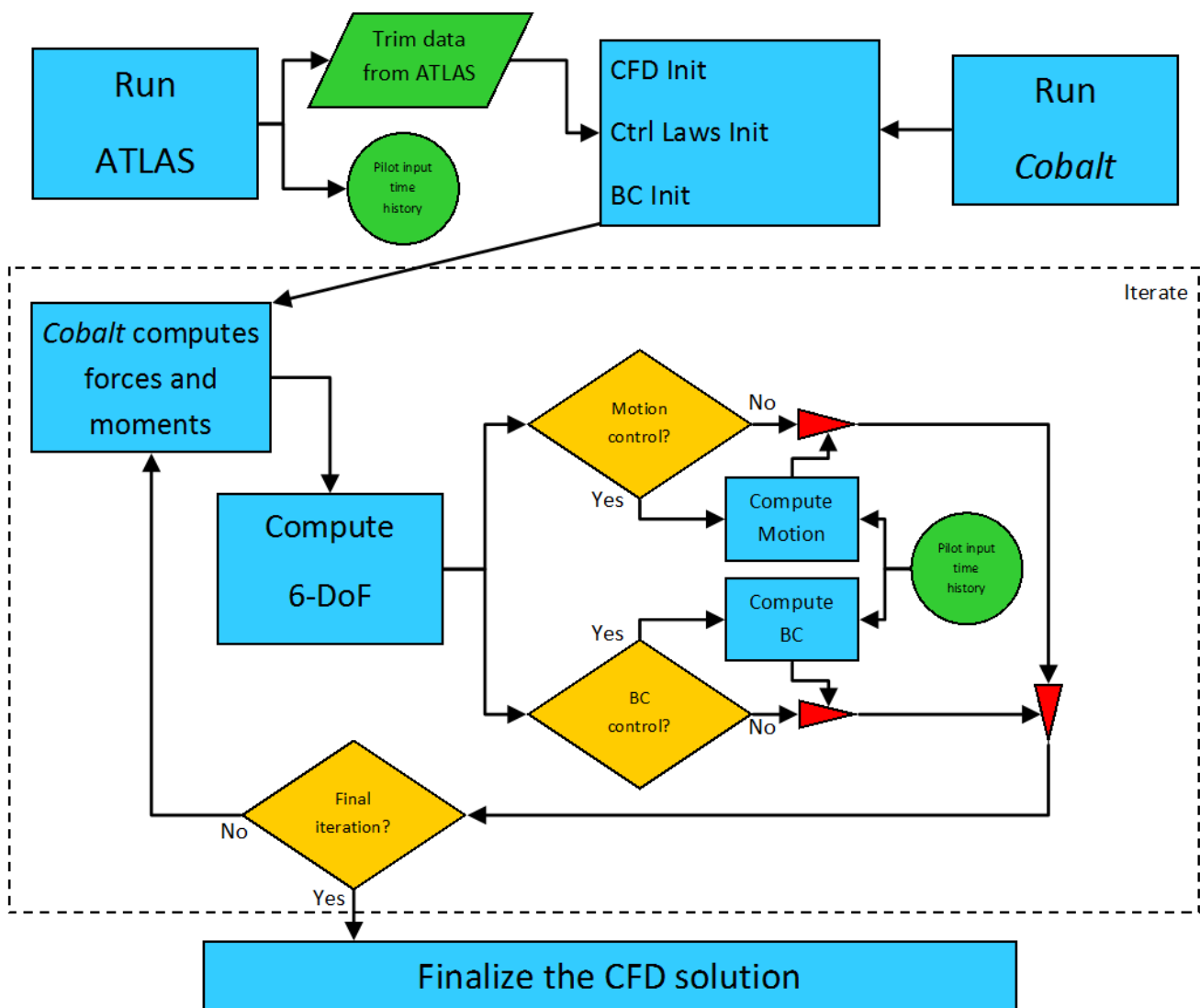


Figure 21. Process of *Cobalt* external feedback control.

Initial testing of the process in Figure 21 has included only motion control of overset grids using external feedback control. Simple sinusoidal motions were commanded via external feedback control to a test grid

including only a main wing and a horizontal tail. In the latest test, both grids moved as expected relative to one another. Work is currently underway modifying the feedback control MATLAB scripts to include BC control and 6-DoF computation.

6. Conclusions

A technique for developing an efficient computational method for accurately determining static and dynamic stability and control (S&C) characteristics of high-performance aircraft as well as the aircraft response to pilot input has been presented. The approach presented herein uses high-fidelity CFD codes run on HPC resources to simulate the response of an aircraft to prescribed motions, which are specifically designed to take full advantage of the unique capabilities of the CFD environment while minimizing the computational time. Multiple example cases have been presented to illustrate that static, unsteady, time-accurate CFD results are comparable to wind tunnel and Lockheed Martin validation data for USAF fighter aircraft in multiple store configurations at subsonic, transonic and supersonic conditions from low to high angles of attack and sideslip.

Discrepancies between CFD and validation data have been identified, particularly aerodynamic moments in both static and dynamic cases. Rigid-body, time-accurate, prescribed motion flight test maneuvers created with the ATLAS software have been performed using the CFD solver *Cobalt*. Prescribed motion moving control surface simulations of the clean F-16 have been performed using *Cobalt* and overset grids. Results have been validated against Lockheed Martin aerodynamic data. It is also shown that static and dynamic aerodynamic coefficients can be determined using SID of CFD simulations for both clean aircraft and aircraft with stores [21]. The nonlinear parametric models identified in this paper provided an excellent fit to the CFD training data. CFD generated models for force coefficients achieved excellent results, whereas moment coefficients earned mixed results against wind tunnel data, performance data, static, time-accurate CFD results, and prescribed motion flight test maneuvers that were not used to create the models. Studies addressing variances in force and moment coefficients, derivatives and their effect on aircraft maneuver response may help quantify the bounds CFD solutions must satisfy and provide guidance to CFD developers on areas in need of improvement. These studies are currently underway. The anticipation is that, through several CFD runs, SID models can be generated that span the aircraft's flight envelope. Once generated, these models can be used to perform a complete matrix of flight test maneuvers in seconds (rather than days or weeks in CFD) as part of a pre-flight check in support of flight test planning and risk reduction. However, highly nonlinear regimes and envelope expansion will still require the performance of complete maneuvers in CFD to refine test plans and reduce test risk and cost.

As confidence in static, unsteady, time-accurate CFD analysis grows, CFD can be used to optimize available test resources and aid clearance of new stores when either test resources or a suitable analogy to previously cleared stores is unavailable. However, the reliability of the CFD solver to produce acceptable results in a timely fashion is paramount to complete integration of CFD into the engineering workflow that supports augmentation of warfighter capability. The criticality of DoD HPC resources is self-evident to perform such analyses in a timely fashion, and highlights the need for continued development and expansion of HPC resources. The capabilities outlined here and those under development represent another step towards the end goal of "flying" an aircraft in CFD, impacting the design phase of the acquisition process and rapidly delivering new capabilities to the warfighter at reduced risk and cost.

Acknowledgments

The computational resources were generously provided by the DoD HPCMP, U.S. Army Engineer Research and Development Center, and Air Force Research Laboratory Department of Defense Shared Resource Center. The authors gratefully acknowledge Dr. Eugene A. Morelli from NASA Langley, who provided the System Identification Programs for Aircraft (SIDPAC), and *COBALT* Solutions for their support. Their work is greatly appreciated.

-
- ¹ M. Withrow, "Dr. Raymond Gordnier Discusses the Research Direction of Advanced Computational Methods," Air Force Research Laboratory Horizons, April 2005.
 - ² J.P. Dean, S.A. Morton, D.R. McDaniel, J.D. Clifton, and D.J. Bodkin, "Aircraft Stability and Control Characteristics Determined by System Identification of CFD Simulations", AIAA Paper 2008-6378, AIAA Atmospheric Flight Mechanics Conference, August 2008, Honolulu, HI.
 - ³ W. Z. Strang, R. F. Tomaro, and M. J. Grismer, "The defining methods of Cobalt60: a parallel, implicit, unstructured Euler/Navier-Stokes flow solver," *AIAA Paper 1999-0786*. 1999.
 - ⁴ R. F. Tomaro, W. Z. Strang, and L. N. Sankar, "An implicit algorithm for solving time dependent flows on unstructured grids," *AIAA Paper 1997-0333*, 1997.
 - ⁵ M. J. Grismer, W. Z. Strang, R. F. Tomaro, and F. C. Witzemman, "Cobalt: A Parallel, Implicit, Unstructured Euler/Navier-Stokes Solver," *Adv. Eng. Software*, Vol. 29, No. 3-6, pp. 365-373, 1998.
 - ⁶ G. Karypis, K. Schloegel, and V. Kumar, "*Parmetis: Parallel Graph Partitioning and Sparse Matrix Ordering Library, Version 3.1*," Technical report, Dept. Computer Science, University of Minnesota, 2003.
 - ⁷ P.R. Spalart, S. Deck, M.L. Shur, K.D. Squires, M.Kh. Strelets, and A. Travin, "A New Version of Detached-Eddy Simulation, Resistant to Ambiguous Grid Densities," *Theoretical Computational Fluid Dynamics*, Vol. 20, pp. 181-195, 2006.
 - ⁸ L. Ljung, "*System Identification. Theory for the User*," Prentice Hall Information and System Sciences Series.
 - ⁹ E. A. Morelli and V. Klein, "Application of System Identification to Aircraft at NASA Langley Research Center," *Journal of Aircraft*, Vol. 42, No. 1, January-February 2005, pp. 12-25.
 - ¹⁰ V. Klein and E. A. Morelli, "*Aircraft System Identification – Theory and Practice*," AIAA Educational Series, 2006.
 - ¹¹ R. V. Jategaonkar, "*Flight Vehicle System Identification – A Time Domain Methodology*," Progress in Astronautics and Aeronautics, Vol. 216, F. K. Lu, editor, AIAA, 2006.
 - ¹² R. V. Jategaonkar, D. Fischenberg, W. Gruenhagen, "Aerodynamic Modeling and System Identification from Flight Data – Recent Applications at DLR," *Journal of Aircraft 2004*, 0021-8669 vol.41 no.4 (681-691), 2004.
 - ¹³ E. A. Morelli, "Global Nonlinear Parametric Modeling with Application to F-16 Aerodynamics," ACC Paper WP04-2, Paper ID i-98010-2, American Control Conference, Philadelphia, Pennsylvania, June 1998.
 - ¹⁴ E. A. Morelli, "System IDentification Programs for AirCRAFT (SIDPAC)," *AIAA Paper 2002-4704*, 2002.
 - ¹⁵ J.P. Dean, J.D. Clifton, D.J. Bodkin, and C.J. Ratcliff, "High Resolution CFD Simulations of Maneuvering Aircraft Using the CREATE-AV/Kestrel Solver", AIAA Paper 2011-1109, 49th AIAA Aerospace Sciences Meeting, 4-7 January 2011, Orlando, Florida.
 - ¹⁶ Gaither, J.A., Marcum, D.L., and Mitchell, B., "SolidMesh: A Solid Modeling Approach to Unstructured Grid Generation," 7th International Conference on Numerical Grid Generation in Computational Field Simulations, 2000.
 - ¹⁷ Marcum, D.L. and Weatherill, N.P., "Unstructured Grid Generation Using Iterative Point Insertion and Local Reconnection," *AIAA Journal*, Vol. 33, No. 9, pp 1619-1625, September 1995.
 - ¹⁸ Marcum, D.L., "Unstructured Grid Generation Using Automatic Point Insertion and Local Reconnection," *The Handbook of Grid Generation*, edited by J.F. Thompson, B. Soni, and N.P. Weatherill, CRC Press, p. 18-1, 1998.
 - ¹⁹ E. A. Morelli, "System IDentification Programs for AirCRAFT (SIDPAC)," *AIAA Paper 2002-4704*, 2002.
 - ²⁰ Miller, Scott H. et al, "Stability and Control Effects of the GBU-39 Small Diameter Bomb (SDB) and BRU-61 Rack on the Block 40 F-16 Aircraft," 16PR18672, Lockheed Martin Aeronautics Company, 21 April 2010.

²¹ Dean, J.P., Clifton, J.D., Bodkin, D.J., Morton, S.A., McDaniel, D.R., "Determining the Applicability and Effectiveness of Current CFD Methods in Store Certification Activities," *AIAA Paper 2010-1231*, AIAA Aerospace Sciences Meeting, Orlando, FL, January 2010